Since January 2020 Elsevier has created a COVID-19 resource centre with free information in English and Mandarin on the novel coronavirus COVID-19. The COVID-19 resource centre is hosted on Elsevier Connect, the company's public news and information website.

Elsevier hereby grants permission to make all its COVID-19-related research that is available on the COVID-19 resource centre - including this research content - immediately available in PubMed Central and other publicly funded repositories, such as the WHO COVID database with rights for unrestricted research re-use and analyses in any form or by any means with acknowledgement of the original source. These permissions are granted for free by Elsevier for as long as the COVID-19 resource centre remains active.

Contents lists available at ScienceDirect

Food and Bioproducts Processing

journal homepage: www.elsevier.com/locate/fbp

Antioxidants entrapment in polycaprolactone microparticles using supercritical assisted injection in a liquid antisolvent

I. Palazzo[a], *P. Trucillo*[a,b], *R. Campardelli*[c,*], *E. Reverchon*[a]

[a] *Department of Industrial Engineering, University of Salerno, Via Giovanni Paolo II, 132 – 84084 Fisciano (SA), Italy*
[b] *Department of Chemical, Material and Industrial Production Engineering, University of Naples Federico II, Piazzale V. Tecchio, 80 – 80125 Napoli, Italy*
[c] *Department of Civil, Chemical and Environmental Engineering (DICCA), University of Genoa, Via Opera Pia 15, 16145 Genova, GE, Italy*

ARTICLE INFO

Article history:
Received 30 April 2020
Received in revised form 10 July 2020
Accepted 14 July 2020
Available online 25 July 2020

Keywords:
Eugenol
α-lipoic acid
Coprecipitates
Supercritical fluids
Antioxidant activity.

ABSTRACT

In this work, the entrapment of two antioxidants, α-lipoic acid (ALA) and eugenol (EUG), in polycaprolactone (PCL) microparticles, using the supercritical assisted injection in a liquid antisolvent (SAILA), is proposed.

Using SAILA, spherical and non-aggregated PCL particles, with average sizes between 0.2 and 1.2 μm, were produced. Then, coprecipitation experiments were performed: PCL/EUG and PCL/ALA particles with an average size of 0.99 ± 0.34 μm and 0.99 ± 0.18 μm, respectively, were produced, with entrapment efficiencies up to 90 %, considerably higher than results reported in the literature. EUG and ALA coprecipitates showed complete release kinetics in a maximum time of 2 days respect to dissolution time of about 4 h and 5 h of unprocessed EUG and ALA, respectively. Furthermore, the antioxidant power of the used compounds was preserved in the obtained co-precipitates.

© 2020 Institution of Chemical Engineers. Published by Elsevier B.V. All rights reserved.

1. Introduction

Antioxidants are widely used as ingredients in food supplements with the aim of maintaining health and preventing illnesses such as cancer and coronary heart disease (Ramaa et al., 2006). Several studies suggested that the integration of antioxidants in the diet has benefits on human health (Barba et al., 2015; Galanakis, 2013) and contributes to the prevention of degenerative diseases (Abdel-Daim et al., 2018). Food bioactives found in traditional Chinese medicine (e.g., plant-derived phenolic compounds, flavonoids from litchi seeds, quercetin, and kaempferol) have been reported to inhibit the enzymatic activity of SARS 3-chymotrypsin-like protease (3CLpro). This enzyme is vital for the replication of SARS-CoV and thus could be suggested as a potential treatment agent against SARS-CoV-2 and supportive care agent for patients with COVID-19 (Galanakis, 2020).

α-Lipoic acid (ALA) and eugenol (EUG) are of particular interest among antioxidant compounds. ALA is a hydrophobic molecule produced by the liver and has documented beneficial effects in the treatment of various diseases, such as hypertension, atherosclerosis, hyperlipidemia, diabetes melli-

Abbreviations: PCL, PolyCaproLactone; SAILA, Supercritical Assisted Injection in a Liquid Antisolvent; EUG, eugenol; ALA, α-lipoic acid; SC-CO_2, Supercritical Carbon Dioxide; PVP, PolyVinylPyrrolidone; SAS, Supercritical AntiSolvent; VLE, Vapor-Liquid Equilibrium; EL, Expanded Liquid; DPPH, 2,2-diphenyl-1-picrylhydrazyl; GLR, Gas to Liquid Ratio; PSD, Particles Size Distribution; DLS, Dynamic Light Scattering; MD, Mean Diameter; SD, Standard Deviation; PDI, PolyDispersity Index; FE-SEM, Field Emission-Scanning Electron Microscope; EA, Ethyl Acetate.

* Corresponding author.
E-mail address: roberta.campardelli@unige.it (R. Campardelli).

https://doi.org/10.1016/j.fbp.2020.07.010
0960-3085/© 2020 Institution of Chemical Engineers. Published by Elsevier B.V. All rights reserved.

tus and in the vascular-cognitive decline associated with aging (Liu, 2008; Zhang et al., 2001). EUG is an aromatic compound, extracted from the essential oil of cloves, used in Chinese and Indian traditional medicine for its digestive, antispasmodic, analgesic, anesthetic, anti-infective, anti-parasitic, tonic and stimulant properties. EUG has shown specific pharmacological and therapeutic activities (Benencia and Courrèges, 2000); EUG is used in dentistry to disinfect dental cavities, to cure caries and to alleviate pain. Other studies showed that EUG has a high antioxidant power and has inhibitory effects on lipid and protein oxidation (Toda, 2003).

However, ALA and EUG are volatile, unstable and sensitive to oxygen, light and heat (Choi et al., 2009; Garg and Singh, 2011; Mourtzinos et al., 2008). Ultrasound (US) treatment was recently indicated as a promising non-conventional processing technologies that can be suitable for preservation of fluid foods. However, the effects of US are usually highly variable, not only according to treatment duration and intensity, but also to the food matrix (Zinoviadou et al., 2015). For these reasons, encapsulation of antioxidants, in this case of ALA and EUG, into drug carriers (Sinha et al., 2001) can be a promising alternative strategy, that can offer numerous benefits such as better stability, protection against oxidation, reduction of toxic effects and better bioavailability (Nedovic et al., 2011; Ramaa et al., 2006; Trujillo Toledo et al., 2016). Attempts to protect antioxidants have been made by encapsulating them in nanoparticles, nanocapsules, microcapsules and liposomes (Woranuch and Yoksan, 2013). In particular, ALA and EUG encapsulation offers many advantages, allowing protection against oxidation and degradation (Loveday and Singh, 2008). The choice of a suitable matrix for encapsulation, generally of polymeric nature, allows to protect and release the drug in a controlled manner (Puttipipatkhachorn et al., 2001).

Industrial scalable approaches have been reported in literature for antioxidant encapsulation; for example, Cortes-Rojas et al. (2014) proposed spray drying for the encapsulation of EUG in solid lipid nanoparticles. The particles were not perfectly spherical and the size distribution was quite wide with particles size at 10, 50 and 90 percentile varying from 2.2 μm to 5.0 μm, from 10.62 μm to 22.49 μm, from 30.54 μm to 48.17 μm, respectively (Cortés-Rojas et al., 2014). However, an increase in the bioavailability of the active ingredient and a good antioxidant activity were observed. Using spray drying, Chatterjee et al. (2013) encapsulated EUG in maltodextrin and arabic gum matrices, obtaining encapsulation efficiencies of 65 % and an encapsulated active principle with potential antioxidant activity, as confirmed by biochemical assays (Chatterjee and Bhattacharjee, 2013). However, the obtained particles were irregular and cohesive.

Shinde et al. (2011) demonstrated the possibility to encapsulate EUG in microcapsules of gelatin-sodium alginate using the coacervation technique induced by a pH change. However, the subsequent treatment with a dehydrating agent caused a shrinkage of the microcapsules with formation of cracks on their surface and consequently a reduction of the encapsulation efficiency (Shinde and Nagarsenker, 2011).

Some authors reported ALA encapsulation in microspheres, using chitosan as the polymeric matrix (Weerakody et al., 2008); using spray-drying process, micrometric ALA-loaded particles with an encapsulation efficiency of 55 % were obtained. However, a reduction of antioxidant activity of ALA of 25 % after encapsulation in the chitosan matrix was observed.

A valid alternative to conventional micronization techniques is represented by supercritical fluid assisted processes, which are widely used to entrap drugs in polymeric matrices (Di Capua et al., 2017a, b; Gimenez-Rota et al., 2019; Tirado et al., 2019). Ozkan et al. (2019) studied the micronization of two flavonoids, quercetin and rutin, and their coprecipitation with polyvinylpyrrolidone (PVP) using the supercritical antisolvent process (SAS). Spherical microparticles were precipitated with entrapment efficiency in PVP of 99.8 % for both flavoinds and the dissolution rate of the coprecipitated powders was 10 and 3.19 times faster compared to the dissolution rates of unprocessed flavonoids (Ozkan et al., 2019).

Supercritical assisted injection in a liquid antisolvent (SAILA) is based on the continuous injection of an expanded liquid formed by an organic solvent, a solute and supercritical carbon dioxide (SC-CO_2)in an antisolvent solution (Campardelli and Reverchon, 2017). In this process, the solvent and the antisolvent phases have to be completely miscible and the solute has to be soluble in the solvent, but not in the antisolvent. A near-equilibrium solution formed by solute, solvent and CO_2 is produced in a saturator filled with packing elements and, then, it is sprayed through a thin wall injector into the precipitation vessel containing water and a surfactant, used as antisolvent. The mixing between the two fluids produces particles precipitation due to the rapid supersaturation. The reasons that make this process advantageous in the production of coprecipitates are related to the possibility of using nontoxic solvents (for example acetone and ethanol), reaching submicronic and nanometric dimensions and producing micro and nanocomposites directly in stable suspensions, with a continuous process in which the particles are obtained in a single step. This process was successfully used to micronize and coprecipitate polymers and pharmaceutical compounds with the production of polymer/drug suspensions (Palazzo et al., 2019; Trucillo and Campardelli, 2019). In particular, SAILA process gave interesting results in the micronization of polycaprolactone (PCL) used as model polymer: particles of about 64 nm, spherical-shaped, monodisperse and non-aggregated were produced (Campardelli et al., 2012).

Poly-ε-coprolactones (PCLs) are polymers of great interest also because they can be easily obtained from non-expensive raw materials (Kwon and Furgeson, 2007). At low molecular weight, they have a semicrystalline structure: the tortuosity of the crystalline form makes PCLs less accessible to water and therefore gives them a lower biodegradability and a low permeability to drugs (Sisson et al., 2013).

The aim of this work is the encapsulation study of antioxidant compounds and in particular ALA and EUG, in a biodegradable and biocompatible polymer, polycaprolactone (PCL). Operating parameters for the coprecipitation of ALA/PCL and EUG/PCL will be studied. The effect of process parameters on particle size distribution and entrapment efficiency will be systematically analyzed. Dissolution tests will be performed to characterize coprecipitates. Moreover, the scavenging activity of the composite compound will be measured and compared with the untreated antioxidant.

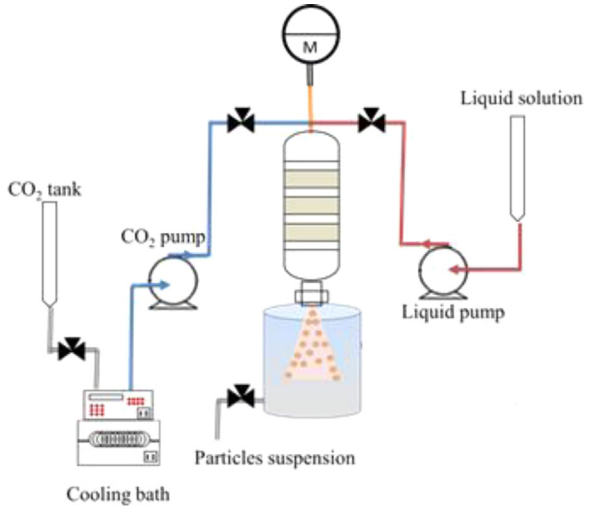

Fig. 1 – SAILA process layout.

2. Materials, apparatus and methods

2.1. Materials

Carbon dioxide, CO_2, was provided by Morlando Group (Naples, Italy). Polysorbate (Tween 80, Sigma Aldrich Chemical Co., Milan, Italy), acetone (AC, purity 99.9 %, Sigma Aldrich Chemical Co., Milan, Italy), ethyl acetate (EA, purity 98 %, Sigma Aldrich Chemical Co., Milan, Italy), 2,2-diphenyl-1-picrylhydrazyl (DPPH, Sigma Aldrich Chemical Co., Milan, Italy), as well as polycaprolactone (PCL, Mw = 14,000 Da), eugenol (EUG) and α-lipoic acid (ALA) were purchased from Sigma (Sigma–Aldrich, St. Louis, USA). All reagents were used as received.

2.2. Apparatus

In SAILA apparatus, supercritical CO_2 and liquid solvent are delivered to a mixer (Fig. 1) (internal volume of 0.15 dm^3) packed with stainless steel perforated saddles and thermally heated by thin band heaters.

Carbon dioxide is cooled using a cooling bath, pumped (Lewa Eco, model LDC-M-2, Italy), preheated and then injected in the mixer. The liquid solution, composed by polymer + solute (drug) and an organic solvent, is pumped using a piston pump (Gilson, model 305, France). SC-CO_2 is continuously solubilized in the liquid solution, forming an expanded liquid (EL). The position of the operating point in the vapor-liquid equilibrium diagram (VLE) of the system CO_2-organic solvent depends on the selected operating conditions of temperature, pressure and on gas to liquid ratio (GLR), i.e., the ratio between CO_2 flow rate and solvent solution flow rate, expressed as weight ratio. The obtained solution is then injected in the precipitation vessel through a micrometric nozzle (80 μm diameter). In the vessel, an antisolvent phase, typically water containing a surfactant is loaded. The solvent/antisolvent ratio was set at 1/4.

2.3. Methods

2.3.1. Particles diameter

Particles size distribution (PSD) of the produced suspensions was obtained using dynamic light scattering (DLS) (Zetasizer, mod. 5000, Malvern Instruments Ltd, UK). Mean diameter (MD), standard deviation (SD) and polydispersity index (PDI) of the particles were measured for each sample. All analysis were carried out in triplicates without any dilution.

2.3.2. Particles morphology

Particle morphology was verified using a field emission-scanning electron microscope (FE-SEM, LEO 1525, Carl Zeiss SMT AG). Recovered suspensions were centrifuged at 6500 rpm for 20 min at −4 °C (Thermo Scientific, mod. IEC CL30R) and particles filtered using membranes with a pore size of 0.2−0.45 μm (Millipore MF membrane filter, Filter type 0.2 μm HA, Sigma Aldrich Chemical Co., Milan, Italy). To perform FE-SEM analysis, powders were coated with a gold layer, using a sputter coater (thickness 250 Å, model B7341; Agar Scientific, Stansted, UK).

2.4. Entrapment efficiency and dissolution tests

The entrapment efficiency was measured dissolving 5 mg of dried particles in 3 mL of ethyl acetate (EA) and measuring the absorbance of the solution at 280 nm for EUG and 325 nm for ALA. Using a calibration curve for each drug (EUG: Abs =0.0142 ppm; ALA: Abs=0.0007 ppm with R^2 = 0.999), the value of absorbance was converted into concentration and then into mass, according to the Lambert-Beer law. The entrapment efficiency (*EE*, %) was calculated as the ratio between the measured (wMA) and theoretical (wTA) antioxidant contents (loaded to the plant), as indicated in the following equation:

$$EE = \frac{wMA}{wTA}100 \quad (1)$$

Dissolution tests of EUG were performed by suspending 20 mg of coprecipitated particles in 3 mL of distillated water and charging the suspension in a dialysis sack (MW cut off 124/174 kDa). EUG coprecipitated particles were put in 250 mL of distillated water continuously agitated at 200 rpm and 37 °C. The concentration of released EUG was continuously monitored measuring the absorbance at 350 nm (UV–vis mod. Cary 50, Varian, Inc., UK).

In the case of ALA loaded particles, 20 mg of the obtained coprecipitates were dispersed in 3 mL of an ethanol/water solution (30:70, v/v) according to Della Porta et al. (2011) protocol (Della Porta et al., 2011). The suspension was introduced into a dialysis sack (MW cut off 124/174 kDa), immersed in 250 mL of ethanol/water solution at 37 °C, and stirred at 200 rpm. The concentration of the active ingredient was continuously monitored using an UV probe at a wavelength of 325 nm. All analyses were performed in triplicate. Dissolution test of unprocessed compounds were also performed.

2.5. Antioxidant activity

The evaluation of antioxidant activity was carried out using the method of Blois (Blois, 1958) with modifications. 1 mL of each sample prepared at different concentrations in acetone was added to 3 mL of an ethanolic solution of DPPH (1×10^{-4} M). The samples were agitated and placed in the dark for 30 min at room temperature. Then, the absorbance was measured at 517 nm. As a negative control, an ethanolic solution of DPPH (1×10^{-4} M) was used in which the samples were replaced by pure acetone. The antioxidant activity was calculated on the basis of the decrease in absorbance that is

Table 1 – PCL precipitation SAILA tests performed at different PCL concentrations in acetone solution. Mean diameter (MD), standard deviation (SD) and polydispersity index (PDI) are also reported.

Test	PCL concentration [mg/mL]	MD ± SD [μm]	PDI
PCL_01	5	1.48 ± 0.57	0.20
PCL_02	10	2.89 ± 0.33	0.27

observed after the radical capture, according to the following equation:

$$\text{Inhibition (\%)} = \left[1 - \frac{A_S}{A_C}\right] 100 \quad (2)$$

where As is the absorbance at 517 nm of the sample treated with DPPH in ethanol solution, and Ac is the negative control absorbance at 517 nm. The scavenging activity reduction obtained in this way was compared with the one of unprocessed samples, to calculate the decrease of DPPH inhibition capacity between unprocessed and processed samples. All determinations were performed in triplicates.

3. Experimental results

3.1. *Polymer precipitation feasibility experiments*

Operating conditions were selected according to previous coprecipitation work using SAILA (Campardelli et al., 2012). These conditions were first tested for PCL particles production. SAILA process operative conditions were: mixer temperature of 60 °C, nozzle diameter of 80 μm, gas-liquid ratio (GLR, by weight) equal to 1.5, CO_2 flow rate 10 g/min. Operative pressure was set at 100 bar for all experiments.

Two tests were carried out with PCL concentrations in acetone of 5 and 10 mg/mL. The anti-solvent phase consisted of 400 mL of distilled water to which Tween 80 has been added, in a percentage of 0.2 % by weight. The surfactant should avoid aggregation phenomena and guarantee a good stability of the microparticles in the aqueous suspension (Zimmermann et al., 2009).

Micrometric particles were obtained in both cases, as shown in Table 1. It can be observed that increasing the concentration of polymer in the organic solvent from 5 to 10 mg/mL, larger particles can be obtained, with diameter of 1.48 ± 0.57 μm and 2.89 ± 0.33 μm, respectively. This effect was due to nucleation and growth of particles as a consequence of supersaturation generated by the antisolvent effect, as reported in literature (Campardelli et al., 2016). Increasing the solute concentration, an increase of nucleation rate occurs, but a large increase of solute concentration produced aggregation of nuclei and then larger particles.

In Fig. 2, SEM images of the produced particles are reported.

FE-SEM images reported in Fig. 2 show that particles produced by SAILA are spherical and with a regular surface. The particles obtained working at the concentration of 5 mg/mL of PCL in acetone are more uniform and regular; for this reason, this polymer concentration was used for antioxidant loading tests.

3.2. *Coprecipitation studies*

The effect of the operating temperature and antioxidant/polymer ratios was studied, setting the polymer concentration in the solution at 5 mg/mL. Process parameters were left unchanged with respect to polymer precipitation feasibility experiments. Experiments were performed for EUG and ALA. Submicro- and microparticles were successfully obtained in all experiments, as shown in Table 2.

The first test was carried out by preparing the solvent solution with 5 % by weight of EUG with respect to the polymer; an homogeneous and stable suspension was obtained. In particular, particles with mean diameter of 0.60 ± 0.18 μm were obtained. Morphological analyses were carried out in order to verify that, in such conditions, co-precipitation of polymer and drug was obtained with consequent formation of composite particles. FE-SEM analysis and entrapment efficiency study revealed that, at these operating conditions, the microparticles are spherical, as shown in Fig. 3a, and the active compound was encapsulated in the polymer matrix with an efficiency of 79.39 %, as reported in Table 2. The co-precipitation of PCL and EUG was therefore successful.

In a next step, the amount of loaded drug was increased to 10 % (w/w). It is possible to note that the mean diameter of the particles increased, and particles with spherical shape and submicrometric dimensions (0.76 ± 0.15 μm) were produced. In this case, eugenol was entrapped in the polymer matrix with a lower entrapment efficiency of 43.15 %.

When the drug/polymer solution at a theorical EUG loading of 20 % (w/w) was processed, the co-precipitation occurred even if there was a worse control of the particle size distribution. Indeed, increasing the percentage of drug loaded particle size distribution was characterized by particles of mean diameter of 0.94 ± 0.55 μm and polydispersion index of 0.58. Entrapment efficiency was further reduced compared to the 5 and 10 % tests, being approximately 21 %.

When the concentration of the antioxidant in the solvent solution increased, the overall effect observed was a reduction of EE with a larger loss of antioxidant in the antisolvent, in which it is partially soluble (solubility of EUG in water of 2.46 mg/mL at room temperature).

A temperature optimization study was also carried out varying the drug/polymer ratio to 5 %, 10 % and 20 % by weight. Temperature used was set at 40 °C, since the entrapment at low temperatures is generally more suitable for the processing of sensitive compounds such as antioxidants. Working at a temperature of 40 °C, the same trend discussed for the tests at 60 °C was observed. As shown in Table 2, the mean diameter slightly increased as the drug/polymer ratio increased, as well as the amplitude of the particle size distribution. Furthermore, the particles produced at 40 °C (Fig. 3b) showed a larger mean size than those obtained at 60 °C (Fig. 3a).

In the SAILA process, the increase of the injection temperature generally produce a reduction in the particles size (Campardelli et al., 2012). This effect is mainly due to the reduction of the surface tension of the expanded liquid, obtained by increasing the temperature. Lower surface tension of the expanded liquid (Cardoso et al., 2008) results in an improvement in the mixing with the antisolvent, which consequently produces smaller particles. In summary, the increase in temperature favours supersaturation and, therefore, a faster precipitation process. Therefore, the particles obtained at 60 °C are characterized by a smaller average size than those produced at 40 °C, as reported in the granulometric curves in Fig. 4.

The entrapment efficiency of the set of experiments performed at 40 °C is similar to that obtained at 60 °C; indeed, when the percentage of the drug load increased from 5 to 20

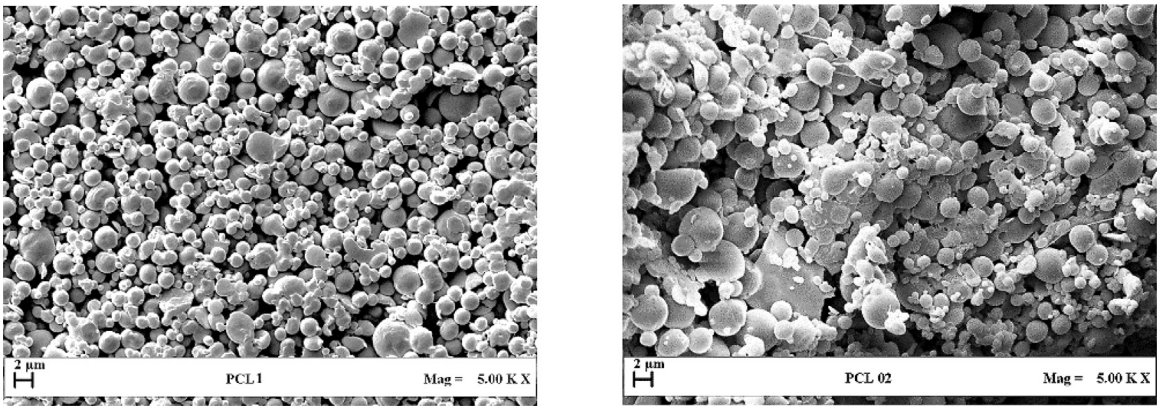

Fig. 2 – FE-SEM of PCL particles obtained at different polymer concentration: (a) 5 mg/mL and (b) 10 mg/mL.

Table 2 – SAILA experiments performed on antioxidant/PCL mixtures using acetone as solvent, setting the polymer concentration at 5 mg/mL for each test and changing the antioxidant/polymer ratio and operating temperature.

Test	Drug/carrier [%]	T [°C]	MD ± SD [μm]	PDI	EE [%]
Eug_01	5	60	0.60 ± 0.18	0.31	79.39
Eug_02	10	60	0.76 ± 0.15	0.20	43.15
Eug_03	20	60	0.94 ± 0.55	0.58	21.05
Eug_04	5	40	0.99 ± 0.34	0.34	94.98
Eug_05	10	40	1.01 ± 0.45	0.44	82.48
Eug_06	20	40	1.26 ± 0.81	0.65	37.94
ALA_01	5	60	0.99 ± 0.25	0.25	78.37
ALA_02	10	60	0.61 ± 0.16	0.26	59.76
ALA_03	20	60	0.54 ± 0.08	0.15	56.24
ALA_04	5	40	0.99 ± 0.18	0.19	93.02
ALA_05	10	40	0.89 ± 0.22	0.25	74.43
ALA_06	20	40	0.79 ± 0.24	0.31	58.57

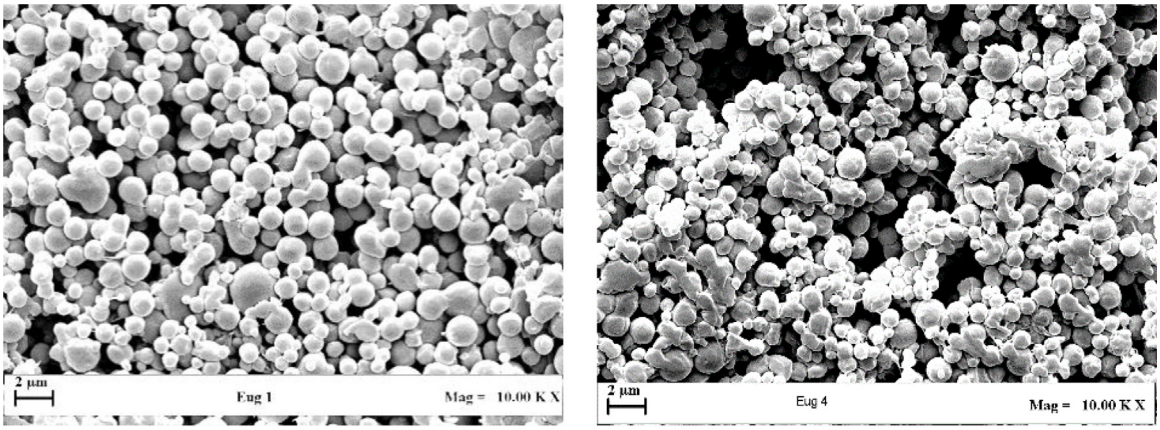

Fig. 3 – FE-SEM images of EUG/PCL particles produced using drug/polymer ratio at 5 % (w/w) and different temperature 60 °C (a) and 40 °C (b), at 100 bar, polymer concentration 5 mg/mL, GLR 1.5, CO_2 flow rate 10 g/min.

%, a progressive decrease of the EE of EUG was obtained, with values of 95, 82 and 38 %, respectively. However, it is possible to note an increase in the entrapment efficiency with respect to the tests performed at a lower temperature from as compared in Fig. 5. This figure shows that the EE increases as the temperature decreases and also it increases as the percentage of antioxidant loading decreases. The positive effect of the temperature reduction on the entrapment efficiency of EUG could be due to a lower loss of the drug in the antisolvent phase. Indeed, during precipitation, EUG tends to diffuse towards the antisolvent phase, in which it has a reduced but however not negligible solubility. At lower temperatures, the solubility of the drug in the antisolvent is lower (~1 mg/mL at 40 °C and 2.4 mg/mL at 60 °C) and, therefore, active principle diffusion in the antisolvent is reduced, resulting in larger entrapment efficiency.

Regarding the effect of drug to polymer ratio on mass basis, a lower percentage of antioxidant loading corresponds to a higher entrapment efficiency, because in SAILA process the co-precipitation takes place following a phenomenon of polymer wrapping around the molecules of drug. At lower drug loading rates, there are many polymer molecules than those of the active ingredient and physical entrapment is facilitated.

Using ALA as antioxidant in the coprecipitation tests, the effect of the operating temperature and the drug loading percentage were repeated. The same experimental proce-

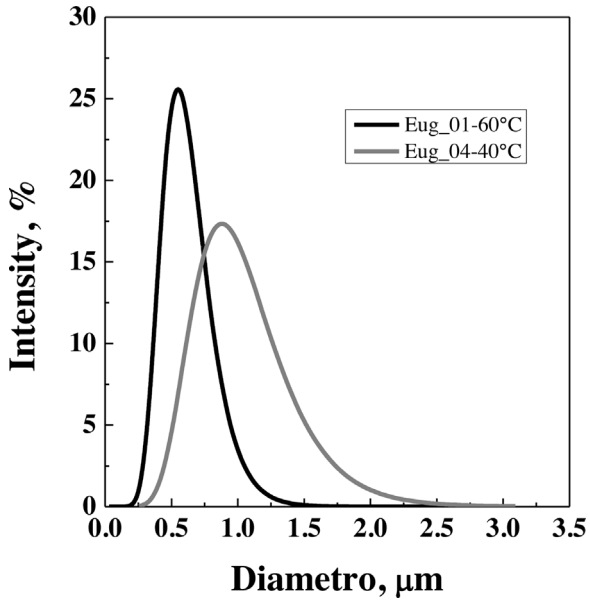

Fig. 4 – Particle size distribution of the tests conducted at 60 °C and 40 °C with EUG with a drug/polymer ratio 5 %.

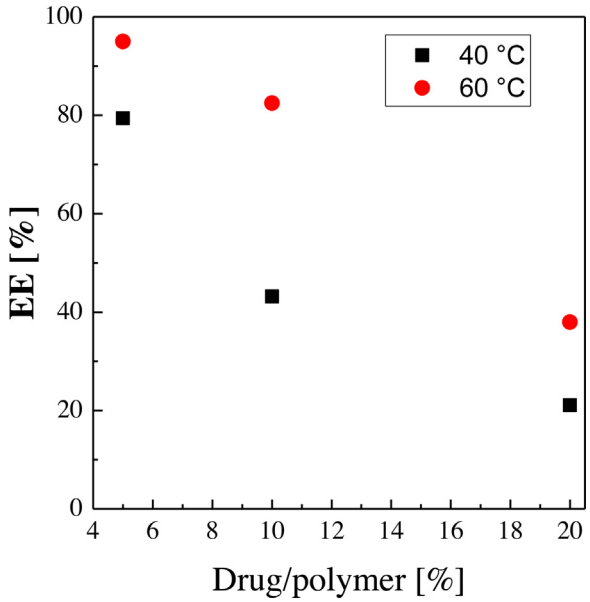

Fig. 5 – Trend of EUG entrapment efficiency (*EE*) vs drug/polymer ratio and temperature.

dure with respect to EUG coprecipitation was carried out: an opaque, homogeneous and stable suspension was obtained using drug/polymer ratio of 5 % by weight.

Morphological analysis at SEM (Fig. 6a) showed that, at these operating conditions, the obtained microparticles are spherical and with an average diameter of about 0.99 ± 0.25 μm. The active compound was encapsulated in the polymeric matrix with an efficiency of 78 %, as reported in Table 2. Increasing drug concentration in the test (ALA_02), the average particle size decreased with values of 0.61 ± 0.16 μm, as reported in Table 2. FE-SEM images (Fig. 6b) show irregular and spherical microparticles; indeed, comparing to the test performed at lower ALA concentration, the antioxidant has been entrapped in the polymeric matrix with a lower encapsulation efficiency, equal to 58 % (see Table 2).

ALA_03 test was performed using the drug/polymer ratio set at 20 %: a reduction in the size of the obtained particles was observed, down to 0.54 ± 0.08 μm. Also in this case, the co-precipitation occurred, as observed from FE-SEM images (Fig. 6c) but with a lower entrapment efficiency, equal to 56 %.

In this case, the increase of antioxidant cargo has favored a reduction of the average dimensions of the produced particles respect to EUG tests. Probably ALA, that is more liposoluble than EUG, was dispersed in a more homogeneous structure within the polymeric matrix to which it is more similar. The previously observed trend for the entrapment efficiency was confirmed: increasing the concentration of loaded drug, there is a reduction in the entrapment efficiency. This result confirms the general mechanism of coprecipitates formation using this technique, that occurs as a sort of wrapping of the drug molecules by the polymer: lower drug/polymer ratios favours this process.

The tests performed using ALA as antioxidant model also showed larger entrapment efficiencies than EUG/PCL coprecipitation tests. This result could be explained considering the different nature of the two compounds studied; ALA is a poorly water soluble compound; therefore, it tends to have a greater affinity with the polymer, compared to the antisolvent phase. Such behavior would produce a better dispersion of ALA in the polymeric matrix, with a consequent reduction in particles mean size and even larger entrapment efficiency.

The same set of experiments was repeated setting the mixer temperature at 40 °C. In particular, morphological analysis and encapsulation efficiency studies showed that, operating at ALA 5 % by weight, spherical particles (Fig. 6d) with an average diameter of about 0.99 ± 0.18 μm (Table 2) were obtained. The active compound was entrapped in the polymeric matrix with an efficiency of 93 %. PCL and ALA coprecipitation was therefore improved by operating at a lower temperature.

PCL/ALA coprecipitation was obtained also increasing the drug/polymer ratio to 10 % and 2 0 %, and from the morphological and granulometric analyses it was possible to note a progressive reduction in particle mean size (Fig. 6 e–f, Table 2). For the set performed at 40 °C, the average diameter decreases whereas the amplitude of the distribution increases as the percentage of ALA increases. Comparing the results obtained at 60 °C and 40 °C, the particles show similar granulometric distribution curves (Fig. 7), but polydispersity values decrease with temperature, respectively of 0.25 and 0.19 at 60 °C and 40 °C.

In all the studied cases, the encapsulation efficiency increases decreasing temperature and also increases when the drug to polymer ratio increases. The positive effect of temperature reduction on the encapsulation efficiency of ALA, as in the case of EUG, could be due to a lower drug diffusion in the antisolvent phase. During precipitation, part of the active principle tends to diffuse in the antisolvent phase, in which it is soluble, although at very low value (0.12 mg/mL): smaller diffusion guarantees larger encapsulation efficiency. The effect of the loading percentage on the encapsulation efficiency obtained at 40 °C and 60 °C, seems to confirm the coprecipitation mechanism based on the polymer wrapping around the drug, as also discussed for EUG tests.

3.3. *Dissolution tests*

Drug release tests were carried out using the coprecipited particles produced at 40 °C. In particular, setting polymer concentration at 5 mg/mL, the effect of drug/polymer ratio on the releases kinetic was studied and compared with dissolution test of pure compounds (Fig. 8a and b).

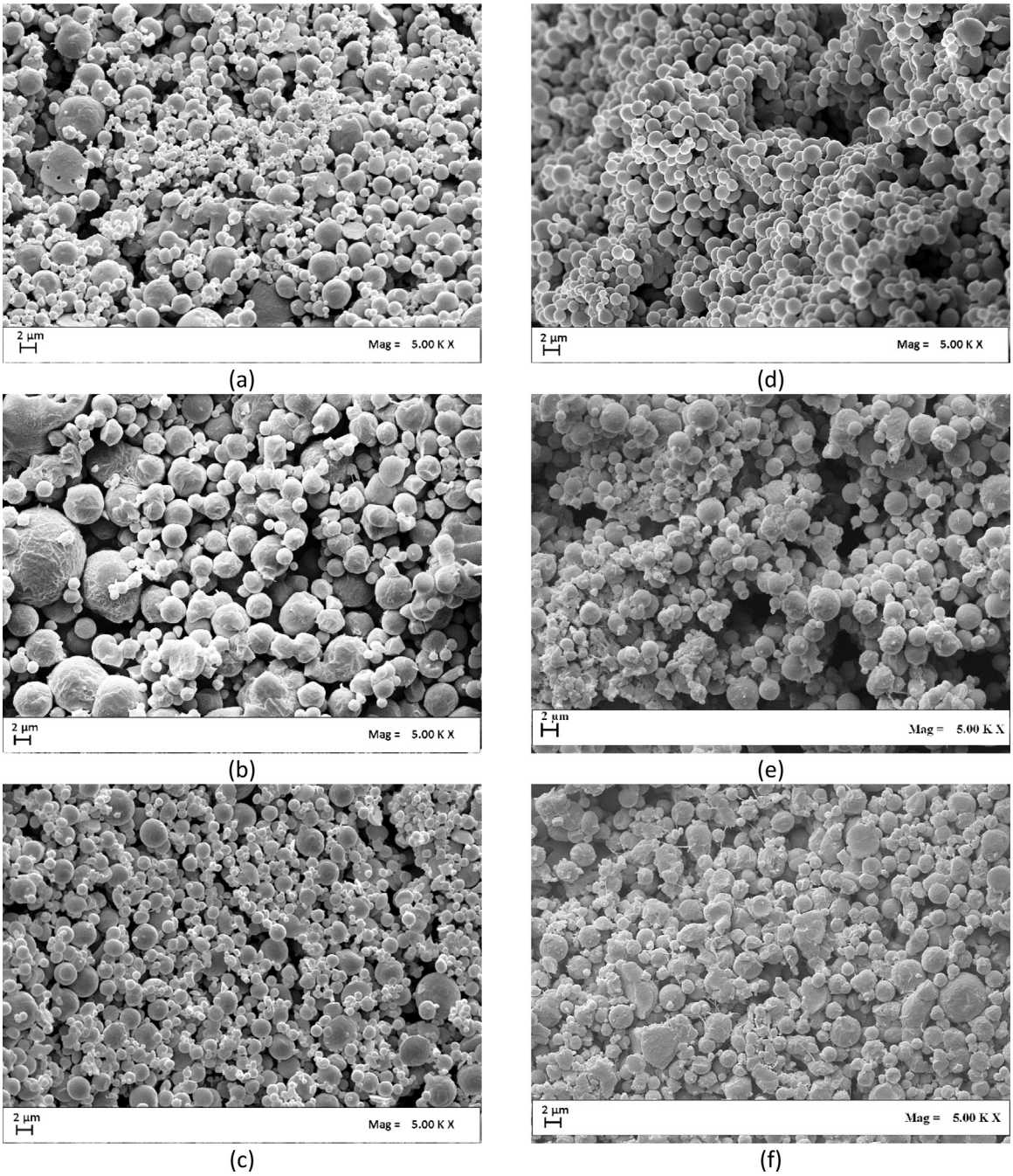

Fig. 6 – FE-SEM images of ALA/PCL particles produced using drug/polymer ratio of 5 % (a, d), 10 % (b, e) and 20 % (c, f) by weight and temperature of 40 °C (a, b, c) and 60 °C (d, e, f), at 100 bar, polymer concentration 5 mg/mL, GLR 1.5, CO_2 flow rate 10 g/min.

Coprecipitates showed slower and controlled release if compared to pure EUG. These results confirm the effective coprecipitation: encapsulated drug emerges from the polymeric matrix through a diffusive mechanism according to a concentration gradient. Particles with larger drug concentration show a slower dissolution time; in particular, Eug_06 shows a release time of about 2 days, whereas for Eug_04, in which there is a smaller amount of drug, the release is completed in a shorter time, about 20 h. This result can be explained considering that, when drug concentration in the polymer is larger than its solubility in the release medium, the diffusive front is very slow because the drug diffuses from the polymer microparticles only when the concentration in the solid phase decreases to a value lower than the equilibrium one. For this reason, higher drug concentration means lower diffusion release. Furthermore, it has to be considered that increasing the drug loading an increase of particles mean diameter was observed, from 0.99 ± 0.34–1.26 ± 0.81 μm. Larger particles are characterized by reduced exposed surface for the release, and therefore by slower release.

Drug presence in the polymeric microparticles was verified also for ALA coprecipitation: in the dissolution test of Fig. 8b, it was possible to verify that the drug is dispersed in the microparticles and it is gradually released. It is possible observe from that figure that particles with a lower concentration of drug show a slower release in the time. In fact, ALA loaded at 5 % by weight shows a release time of about 44 h compared to pure ALA that is completely released after 5 h. In test the sample ALA_05 (loading at 10 %, w/w), loses its

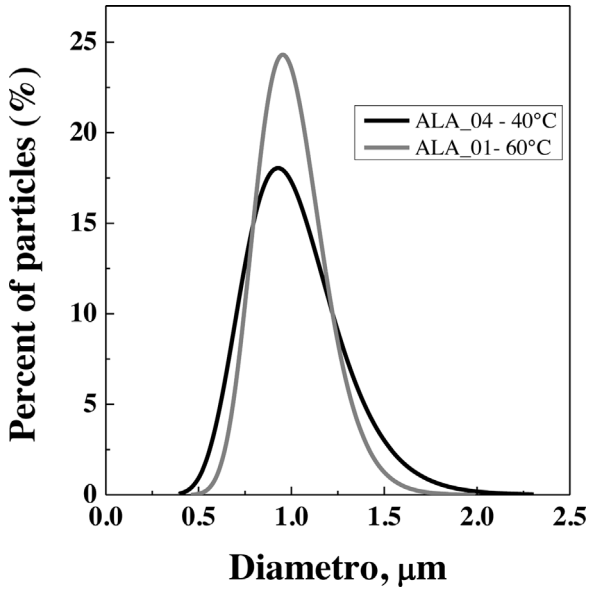

Fig. 7 – Particle size distribution of the tests conducted at 60 °C and 40 °C with ALA with a drug/polymer ratio 5 %.

content after 27 h, and finally the ALA_06 test, in which the largest amount of drug is present (20 % by weight), releases coprecipitated drug in about 19 h. In this last case, therefore, a greater concentration of drug corresponds to a faster dissolution rate. However, these results are not directly comparable with those obtained in the case of EUG because these release kinetics were performed in a modified external medium, in which ethanol was added at 30 % (v/v) to facilitate the dissolution of ALA. Indeed, ALA shows a poor solubility in water, equal to about 0.12 mg/mL at room temperature. Therefore, if released into an aqueous medium, it should require longer observation times. Furthermore, a procedure reported in the literature (Della Porta et al., 2011) has been adopted in order to verify that co-precipitation has occurred and, therefore, that the release was modulated by the presence of the polymer. This procedure involves the use of a modified release medium and is often employed for compounds that have a low solubility in the pure solvent. Also in this case, the release kinetics can be correlated to particles diameters. Indeed, increasing the drug loading, a reduction of particles mean diameters was observed from 0.99 ± 0.18 to 0.79 ± 0.24 μm and, therefore, an increase of the exposed surface area for drug release that could produce an acceleration of drug release at higher drug loading.

Dissolution kinetics of coprecipitated samples produced at different temperature were also studied. Using a polymer concentration of 5 mg/mL and setting the drug weight percentage at 5 % (w/w), microparticles obtained at operative temperature

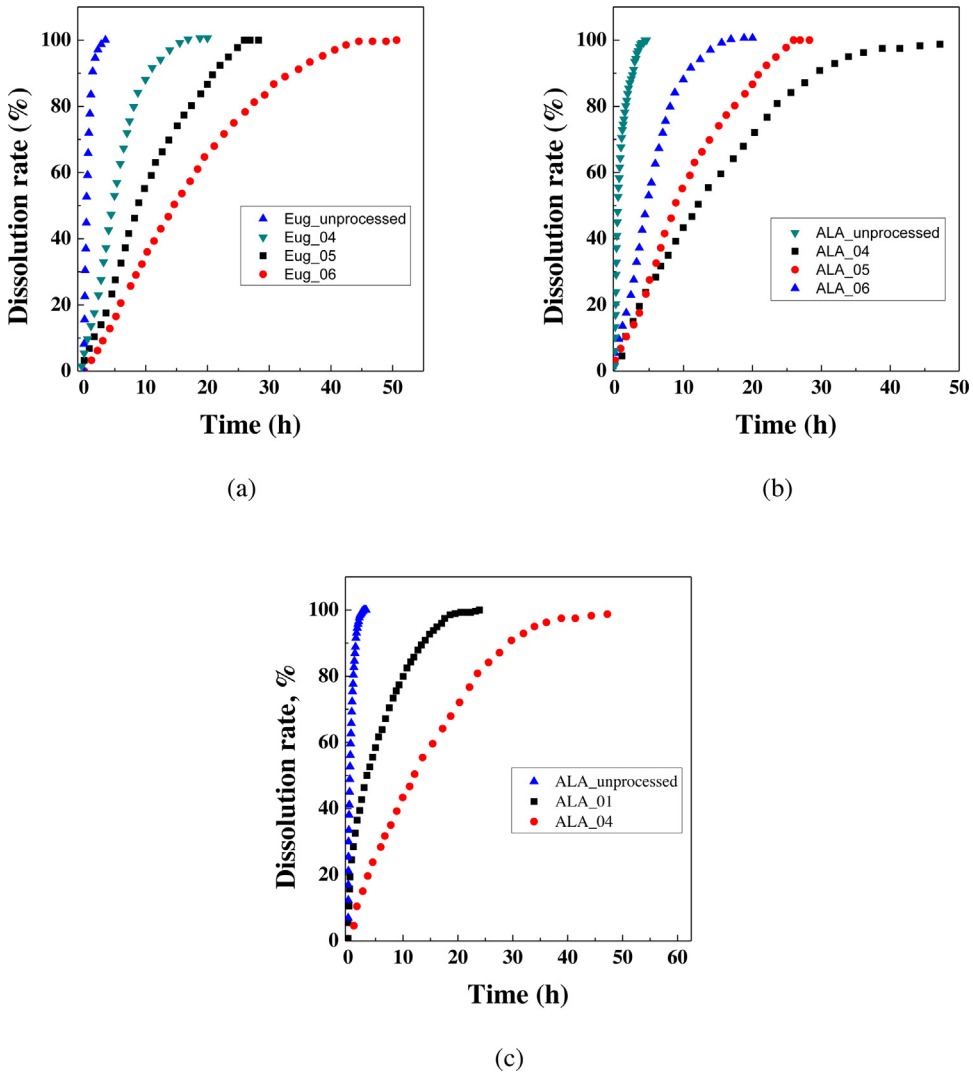

Fig. 8 – Dissolution tests of EUG (a) and ALA (b) at different drug/polymer ratio setting operative temperature 40 °C and dissolution tests of PLC/ALA 20/1 (w/w) at 40 °C and 60 °C (c).

Table 3 – Radical scavenging activity of coprecipitates respect to pure compound with DPPH assay.

Test	Temperature [°C]	% Inhibition (processed)	EE	% Inhibition (pure compound)	% Inhibition reduction
Eug_01	60	50.7	0.79	65.9	23.0
Eug_02	60	41.7	0.43	62.1	32.8
Eug_03	60	42.1	0.21	61.7	31.8
Eug_04	40	71.7	0.95	74.6	3.89
Eug_05	40	73.1	0.82	75.8	3.56
Eug_06	40	57.0	0.38	62.9	9.38
ALA_01	60	56.8	0.78	57.9	1.90
ALA_02	60	54.6	0.60	62.7	12.9
ALA_03	60	75.0	0.56	80.4	6.72
ALA_04	40	54.7	0.93	60.0	8.83
ALA_05	40	57.9	0.74	67.8	14.6
ALA_06	40	81.2	0.59	81.8	0.73

of 60 °C and 40 °C were analyzed and the their release kinetics were reported in Fig. 8c.

Test ALA_04 carried out at 40 °C, shows that all the ALA contained in the microparticles is released in a concentration lower than the test carried out at 60 °C (ALA_01). Furthermore, it should be noted that, when saturator temperature increases, the initial burst in the release is more pronounced; indeed, over 40 % of the drug is released after just 2 h. This trend could be due to the drug presence on the microparticles surface in the case of particles produced at 60 °C and could confirm the hypothesis of the competition of the drug diffusive phenomenon with respect to precipitation in the antisolvent at a higher temperature, as illustrated in a previous coprecipitation study (Palazzo et al., 2019).

3.4. *Antioxidant activity*

Previous characterizations confirmed drug and polymer coprecipitation in the SAILA microparticles, good drug encapsulation efficiencies and release times of the active compound longer than the pure antioxidant.

However, EUG and ALA are very labile antioxidants and their scavenging activity is greatly reduced due to environmental degradation agents such as light or heat; indeed to protect them against oxidation, they were encapsulated in PCL. The radical scavenging activity of the coprecipitates was measured using a spectrophotometric assay (DPPH) in order to determine that the coprecipitation did not result in antioxidants degradation.

The DPPH test was first performed on pure compounds. Samples were prepared dissolving EUG and ALA at different concentrations in acetone and adding at each sample the ethanolic solution of DPPH. The absorbance values obtained were converted in terms of % inhibition, according to the Eq. (2) described in Methods section. Hence, using the same technique, coprecipitated samples were analyzed and the results of the scavenging activity are reported in Table 3. In terms of % inhibition reduction of the processed powder with respect to the pure compounds. In details, DPPH assay on EUG confirms that when the temperature of 40 °C was used, the process did not cause antioxidant degradation. Indeed, there is a small decrease in the inhibition percentage compared to the unprocessed compound and respect the test carried out at 60 °C. On other hand, using ALA, even the temperature of 60 °C had no negative effects on the antioxidant activity of the produced coprecipitates. Probably ALA is less sensitive to temperature than EUG. These results confirm that SAILA coprecipitation did not modify the scavenging activity of the samples and preserve their degradation.

4. Conclusions

SAILA technique was demonstrated to be successful for PCL precipitation and for processing sensitive compounds as antioxidants. Spherical and non aggregated coprecipitated particles were produced in all studied cases. High polymer/antioxidant ratio (20/1) and low operating temperature (40 °C) allowed coprecipitation with high EUG and ALA entrapment efficiency (up to 90 %). EUG and ALA coprecipitates showed slower and controlled dissolution compared to pure compounds. Release kinetics was influenced by the operative temperature: at 40 °C slower dissolution rate was observed, due to higher antioxidant entrapment in the polymer matrix. SAILA coprecipitation preserved the scavenging activity of the used antioxidants. These results allow to consider this novel technique ad an alternative to consolidate micronization processes, such as spray drying or emulsion evaporation, with the advantage of producing directly stabilized suspensions and working at low temperatures.

Declaration of Competing Interest

The authors report no declarations of interest.

Acknowledgments

Authors want to acknowledge Dr. Federica Ferrara for her help in the experimental part for the production of microparticles during her master degree thesis developed at the Department of Industrial Engineering, University of Salerno, Italy.

References

Abdel-Daim, M.M., Zakhary, N.I., Aleya, L., Bungău, S.G., Bohara, R.A., Siddiqi, N.J., 2018. Aging, metabolic, and degenerative disorders: biomedical value of antioxidants. Oxid. Med. Cell. Longev. 2018, 2098123.

Barba, F.J., Galanakis, C.M., Esteve, M.J., Frigola, A., Vorobiev, E., 2015. Potential use of pulsed electric technologies and ultrasounds to improve the recovery of high-added value compounds from blackberries. J. Food Eng. 167, 38–44.

Benencia, F., Courrèges, M.C., 2000. In vitro and in vivo activity of eugenol on human herpesvirus. Phytother. Res. 14, 495–500.

Blois, M.S., 1958. Antioxidant determinations by the use of a stable free radical. Nature 181, 1199–1200.

Campardelli, R., Reverchon, E., 2017. Instantaneous coprecipitation of polymer/drug microparticles using the supercritical assisted injection in a liquid antisolvent. J. Supercrit. Fluids 120, 151–160.
Campardelli, R., Adami, R., Della Porta, G., Reverchon, E., 2012. Nanoparticle precipitation by supercritical assisted injection in a liquid antisolvent. Chem. Eng. J. 192, 246–251.
Campardelli, R., Oleandro, E., Reverchon, E., 2016. Supercritical assisted injection in a liquid antisolvent for PLGA and PLA microparticle production. Powder Technol. 287, 12–19.
Cardoso, M.A.T., Monteiro, G.A., Cardoso, J.P., Prazeres, T.J.V., Figueiredo, J.M.F., Martinho, J.M.G., Cabral, J.M.S., Palavra, A.M.F., 2008. Supercritical antisolvent micronization of minocycline hydrochloride. J. Supercrit. Fluids 44, 238–244.
Chatterjee, D., Bhattacharjee, P., 2013. Comparative evaluation of the antioxidant efficacy of encapsulated and un-encapsulated eugenol-rich clove extracts in soybean oil: shelf-life and frying stability of soybean oil. J. Food Eng. 117, 545–550.
Choi, M., Soottitantawat, A., Nuchuchua, O., Min, S., Ruktanonchai, U., 2009. Physical and light oxidative properties of eugenol encapsulated by molecular inclusion and emulsion-diffusion method. Food Res. Int. 42, 148–156.
Cortés-Rojas, D.F., Claudia, R.F.S., Wanderley, P.O., 2014. Encapsulation of eugenol rich clove extract in solid lipid carriers. J. Food Eng. 127, 34–42.
Della Porta, G., Campardelli, R., Falco, N., Reverchon, E., 2011. PLGA microdevices for retinoids sustained release produced by supercritical emulsion extraction: continuous versus batch operation layouts. J. Pharm. Sci. 100, 4357–4367.
Di Capua, A., Adami, R., Izzo, L., Reverchon, E., 2017a. Luteolin/dextran-FITC fluorescent microspheres produced by supercritical assisted atomization. J. Supercrit. Fluids 130, 97–104.
Di Capua, A., Adami, R., Reverchon, E., 2017b. Production of Luteolin/Biopolymer microspheres by supercritical assisted atomization. Ind. Eng. Chem. Res. 56, 4334–4340.
Galanakis, C.M., 2013. Emerging technologies for the production of nutraceuticals from agricultural by-products: a viewpoint of opportunities and challenges. Food and bioproducts processing : transactions of the Institution of Chemical Engineers, Part C. 91, 575–579.
Galanakis, C.M., 2020. The food systems in the era of the coronavirus (COVID-19) pandemic crisis. Foods 9.
Garg, A., Singh, S., 2011. Enhancement in antifungal activity of eugenol in immunosuppressed rats through lipid nanocarriers. Colloids Surf. B Biointerfaces 87, 280–288.
Gimenez-Rota, C., Palazzo, I., Scognamiglio, M.R., Mainar, A., Reverchon, E., Della Porta, G., 2019. β-Carotene, α-tocoferol and rosmarinic acid encapsulated within PLA/PLGA microcarriers by supercritical emulsion extraction: encapsulation efficiency, drugs shelf-life and antioxidant activity. J. Supercrit. Fluids 146, 199–207.
Kwon, G.S., Furgeson, D.Y., 2007. 4 - biodegradable polymers for drug delivery systems. In: Jenkins, M. (Ed.), Biomedical Polymers. Woodhead Publishing, pp. 83–110.
Liu, J., 2008. The effects and mechanisms of mitochondrial nutrient α-Lipoic acid on improving age-associated mitochondrial and cognitive dysfunction: an overview. Neurochem. Res. 33, 194–203.
Loveday, S., Singh, H., 2008. Recent advances in technologies for Vitamin A protection in foods. Trends Food Sci. Technol. 19, 657–668.
Mourtzinos, I., Kalogeropoulos, N., Papadakis, S.E., Konstantinou, K., Karathanos, V.T., 2008. Encapsulation of nutraceutical monoterpenes in β-Cyclodextrin and modified starch. J. Food Sci. 73, S89–S94.
Nedovic, V., Kalusevic, A., Manojlovic, V., Levic, S., Bugarski, B., 2011. An overview of encapsulation technologies for food applications. Procedia Food Sci. 1, 1806–1815.
Ozkan, G., Franco, P., Capanoglu, E., De Marco, I., 2019. PVP/flavonoid coprecipitation by supercritical antisolvent process. Chem. Eng. Process. Process. Intensif. 146, 107689.
Palazzo, I., Campardelli, R., Scognamiglio, M., Reverchon, E., 2019. Zein/luteolin microparticles formation using a supercritical fluids assisted technique. Powder Technol. 356, 899–908.
Puttipipatkhachorn, S., Nunthanid, J., Yamamoto, K., Peck, G.E., 2001. Drug physical state and drug–polymer interaction on drug release from chitosan matrix films. J. Control. Release 75, 143–153.
Ramaa, C.S., Shirode, A.R., Mundada, A.S., Kadam, V.J., 2006. Nutraceuticals - an emerging era in the treatment and prevention of cardiovascular diseases. Curr. Pharm. Biotechnol. 7, 15–23.
Shinde, U., Nagarsenker, M., 2011. Microencapsulation of eugenol by gelatin-sodium alginate complex coacervation. Indian J. Pharm. Sci. 73, 311–315.
Sinha, J., Das, N., Basu, M.K., 2001. Liposomal antioxidants in combating ischemia-reperfusion injury in rat brain. Biomed. Pharmacother. 55, 264–271.
Sisson, A.L., Ekinci, D., Lendlein, A., 2013. The contemporary role of ε-caprolactone chemistry to create advanced polymer architectures. Polymer 54, 4333–4350.
Tirado, D.F., Palazzo, I., Scognamiglio, M., Calvo, L., Della Porta, G., Reverchon, E., 2019. Astaxanthin encapsulation in ethyl cellulose carriers by continuous supercritical emulsions extraction: a study on particle size, encapsulation efficiency, release profile and antioxidant activity. J. Supercrit. Fluids 150, 128–136.
Toda, S., 2003. Inhibitory effects of aromatic herbs on lipid peroxidation and protein oxidative modification by copper. Phytother. Res. 17, 546–548.
Trucillo, P., Campardelli, R., 2019. Production of solid lipid nanoparticles with a supercritical fluid assisted process. J. Supercrit. Fluids 143, 16–23.
Trujillo Toledo, L., Avalos, R., Granda, S., Guerra, L., Pais Chanfrau, J., 2016. Nanotechnology applications for food and bioprocessing industries. Biol. Med. 8, 3.
Weerakody, R., Fagan, P., Kosaraju, S.L., 2008. Chitosan microspheres for encapsulation of α-lipoic acid. Int. J. Pharm. 357, 213–218.
Woranuch, S., Yoksan, R., 2013. Eugenol-loaded chitosan nanoparticles: I. Thermal stability improvement of eugenol through encapsulation. Carbohydr. Polym. 96, 578–585.
Zhang, L., Xing, G.Q., Barker, J.L., Chang, Y., Maric, D., Ma, W., Li, B.S., Rubinow, D.R., 2001. α-lipoic acid protects rat cortical neurons against cell death induced by amyloid and hydrogen peroxide through the akt signalling pathway. Neurosci. Lett. 312, 125–128.
Zimmermann, A., Millqvist-Fureby, A., Elema, M.R., Hansen, T., Müllertz, A., Hovgaard, L., 2009. Adsorption of pharmaceutical excipients onto microcrystals of siramesine hydrochloride: effects on physicochemical properties. Eur. J. Pharm. Biopharm. 71, 109–116.
Zinoviadou, K.G., Galanakis, C.M., Brnčić, M., Grimi, N., Boussetta, N., Mota, M.J., Saraiva, J.A., Patras, A., Tiwari, B., Barba, F.J., 2015. Fruit juice sonication: implications on food safety and physicochemical and nutritional properties. Food Res. Int. 77, 743–752.